光学学报

超构表面偏振调控最新研究进展(特邀)

许丽佳[1,2,3], 郑宇晗[1,3,4,5], 郭迎辉[1,3,4,5], 蒲明博[1,3,4,5], 李雄[1,3,4], 马晓亮[1,3,4], 罗先刚[1,3,4*]

[1]中国科学院光电技术研究所微细加工光学技术国家重点实验室, 四川 成都 610209;
[2]电子科技大学自动化工程学院, 四川 成都 611731;
[3]中国科学院大学材料科学与光电技术学院, 北京 100049;
[4]中国科学院光场调控科学与技术重点实验室, 四川 成都 610209;
[5]中国科学院光电技术研究所矢量光场研究中心, 四川 成都 610209

摘要 作为光波和电磁波的基本参量之一,偏振态的高效调控是电磁波操纵的核心内容,在成像、通信、显示、光学加密、光力操纵等领域至关重要。超构表面可以在亚波长尺度上操控偏振态,因此成为偏振调控和矢量光束生成的强大工具。本综述首先简单介绍了偏振调控超构表面的基本原理和典型结构,然后重点总结了它在传播方向偏振转换、矢量涡旋光束生成、矢量全息和加密、矢量偏振测量和动态调控等方面的最新应用进展,最后对该领域未来可能的发展方向进行了展望。

关键词 物理光学; 超构表面; 涡旋光; 偏振; 全息; 偏振测量; 动态调控

中图分类号 O436 **文献标志码** A **DOI**: 10.3788/AOS240480

1 引 言

超构材料是一类由特殊设计的微结构单元(也称人工原子或超构原子)构建的人工材料[1-2]。根据所调控的物理特性,超构材料可分为电磁超构材料、力学超构材料、声学超构材料、热学超构材料等。其中,电磁超构材料利用亚波长结构的奇异电磁响应实现了超越自然材料的电磁性能,颠覆了经典光学和电磁学的许多概念[3]。自21世纪初以来,经过二十余年的发展,超构材料已经在电磁隐身与电磁幻象[4-5]、超分辨率成像与光刻[6-7]、异常光学透射[8]等领域展现出广阔的应用前景。然而,三维超构材料存在制备困难、损耗大、难以集成等问题,严重制约了超构材料的深入发展和实际应用。于是,从2010年左右开始,人们将目光投向了超构表面。所谓超构表面(也称超表面),在很多情况下可以认为是将人工电磁微结构按照均匀或非均匀空间排列组成的二维超构材料。超构表面器件加工简单、轻薄、易集成、损耗低,且能够在亚波长尺度调控光场的振幅、相位和偏振,因而受到了越来越多的关注[9-13]。

偏振(在微波领域称为极化)是电磁波重要的基本属性,是指其传播过程中电磁矢量(垂直于波的传播方向)沿着特定方向振动的现象,包括线偏振、圆偏振、椭圆偏振以及更广义的空间非均匀偏振(即矢量光场)。对电磁波偏振状态的高效调控,是光学领域的基本问题[14-16],在通信[17-18]、成像显示[19-21]、遥感[22]等领域至关重要。传统的偏振转换器通常由块体或多层级联的具备旋光性或双折射特性的材料构成,整体结构笨重且调控能力有限。利用单一超构表面同时生成多种不同极化状态的波束,适应于当前光学系统小型化和集成化的发展趋势。

近年来,基于超构表面的偏振调控技术发展迅速。虽然已经有多篇综述系统地阐述了超构表面偏振调控的原理、方法及应用[23-24],但未能涵盖本领域的最新进展。本综述从超构表面偏振调控的基本原理出发,重点总结了偏振调控超构表面的一些新兴应用,包括传播方向偏振转换、矢量涡旋光束生成、矢量全息和加密、矢量偏振测量和动态调控等。

2 偏振调控超构表面的原理与典型结构

传统的体偏振调控器(包括自然材料、三维超构材料等)通常借助电磁波在其体内的"传输相位"进行光学操控,控制的是光的全局偏振。与之不同的是,超构表面是利用其界面上的各向异性反射/透射时的"相位突变"实现偏振和波前的调控。"相位突变"属于

收稿日期: 2024-01-11; **修回日期**: 2024-02-21; **录用日期**: 2024-02-22; **网络首发日期**: 2024-03-13

基金项目: 国家重点研发计划(2018YFA0701800, 2021YFA1401003)、国家自然科学基金(62222513, 61975210)、四川省科技计划项目(2020YFJ0001)

通信作者: *lxg@ioe.ac.cn

表面效应，根据产生机理的不同可以分为几何(Pancharatnam Berry)相位[25]、传输相位[26]、界面相位[27]、广义几何相位[28]等。若将具有不同突变相位的人工原子集成到一块平面材料，获得非均匀的相位分布，且相位函数依赖于位置、时间，以及入射波的偏振，则可以在纳米尺度上实现对电磁波的逐点偏振转换，从而产生矢量光场[29-30]。

下面基于琼斯矩阵介绍超构表面偏振调控的基本原理。一般而言，输入和输出光场之间的关系可以表示为 $\boldsymbol{E}^{\text{out}}=\boldsymbol{J}\boldsymbol{E}^{\text{in}}$，其中，$\boldsymbol{E}^{\text{in}}$ 表示具有空间变化电场的入射光波，$\boldsymbol{E}^{\text{out}}$ 表示所需要的输出电场。假设各向异性结构对应 u-v 坐标系，整个超构表面对应为 x-y 坐标系，两个坐标系的夹角为 θ。各向异性超构原子的琼斯矩阵通过特征分解，得到

$$\boldsymbol{J}=\boldsymbol{R}(\theta)\begin{bmatrix} t_u & 0 \\ 0 & t_v \end{bmatrix}\boldsymbol{R}(-\theta),\tag{1}$$

式中：t_u 和 t_v 分别为入射光沿超构原子两个轴线方向的复振幅，由超构原子沿两轴的尺寸决定；$\boldsymbol{R}(\theta)$ 为旋转矩阵，

$$\boldsymbol{R}(\theta)=\begin{bmatrix} \cos\theta & \sin\theta \\ -\sin\theta & \cos\theta \end{bmatrix}。\tag{2}$$

因此，琼斯矩阵的两组特征值 λ_i 和特征向量 $\boldsymbol{x}_i$ 分别为 $\lambda_1=t_u$、$\boldsymbol{x}_1=\begin{bmatrix} \cos\theta \\ -\sin\theta \end{bmatrix}$，$\lambda_2=t_v$、$\boldsymbol{x}_2=\begin{bmatrix} \sin\theta \\ \cos\theta \end{bmatrix}$。

传统超构表面偏振调控的重要方式之一是几何相位，其机理是光子的自旋-轨道相互作用(PSOI)，对应于式(2)的旋转矩阵。具体而言，如果均匀偏振波前的两部分沿着庞加莱球面上的两条不同路径传输到共同的偏振态，则二者之间会出现一个相对相位，该相位等于路径所围成的半个立体角。因此，当圆偏振光束 $\boldsymbol{E}^{\text{in}}=\begin{bmatrix} 1 \\ \pm\mathrm{i} \end{bmatrix}$ 通过超构表面时，根据式(1)，将琼斯矩阵相乘可得输出光[23]：

$$\boldsymbol{E}^{\text{out}}=\boldsymbol{J}\boldsymbol{E}^{\text{in}}=\frac{t_u+t_v}{2}\begin{bmatrix} 1 \\ \pm\mathrm{i} \end{bmatrix}+\frac{t_u-t_v}{2}\exp(\mp\mathrm{i}2\theta)\begin{bmatrix} 1 \\ \mp\mathrm{i} \end{bmatrix}。\tag{3}$$

方程右边第一项表示与入射光具有相同手性的圆偏振光波，第二项表示与入射光具有相反手性的圆偏振光波且带有一个额外的几何相位 2θ。例如，对于由半波片单元组成的超构表面，式(3)中只保留第二项，其角向 θ 在空间范围内变化，可以在其中一个圆极化上施加一个相位轮廓 $\varphi(x,y)=2\theta(x,y)$。如果超构原子从0旋转到π，其几何相位从0线性增加到2π。然而，以这种方式对左旋圆偏振(LCP)和右旋圆偏振(RCP)光施加的相位是共轭对称的，即 $\varphi_{\text{LCP}}(x,y)=-\varphi_{\text{RCP}}(x,y)$。

除了几何相位，传播相位也可以用来实现偏振操控。如果超构原子保持其角度方向 θ 不变，则式(1)中的琼斯矩阵可简化为

$$\boldsymbol{J}=\begin{bmatrix} \mathrm{e}^{\mathrm{i}\varphi_x} & 0 \\ 0 & \mathrm{e}^{\mathrm{i}\varphi_y} \end{bmatrix},\tag{4}$$

式中：φ_x 和 φ_y 表示光沿其两轴的传播相移。这意味着在 x 和 y 线偏振光作用下，输出电场可以分别由 $\begin{bmatrix} \mathrm{e}^{\mathrm{i}\varphi_x} \\ 0 \end{bmatrix}$ 和 $\begin{bmatrix} 0 \\ \mathrm{e}^{\mathrm{i}\varphi_y} \end{bmatrix}$ 获得。因此，传播相位设计通过调整单元的形状，允许在两个正交的线偏振光上分别施加独立和任意的相位轮廓。

综上所述，根据式(1)和式(2)，利用一个至少有3个参数的超构表面，只要其 t_u 和 t_v 以及面内方位角 θ 可以自由设计，就可以得到任意对称且实正交的琼斯矩阵，从而实现完全的偏振和相位控制[31]。这种独立调控方法显著扩展了超构表面偏振光学的范围，为矢量涡旋光束的产生、更复杂的复用元件的应用提供了任意相位分布。

图1简要总结了偏振调控超构表面的发展路线。早期的尝试通常依赖于偏振光栅结构。Hasman团队最早提出一种全介质型亚波长微条纹光栅结构超构表面[图1(a)]，在10.6 μm 波长实现了几何相位调制[32]和矢量光束产生[33]。随后，许多基于几何相位的超构表面创造出奇异的结构光场[34-36]。特别是2015年提出的悬链线结构[图1(c)]，可以解决Hasman团队所采用的方法中存在的"相位复杂度高和空间尺寸受限问题"，实现不受限制的连续高效率几何相位调控[37]。

另一种经典结构是具有金属-绝缘体-金属(MIM)结构的超反射镜[38-40][图1(b)]。基于电路型相位调控原理，该结构对相位的调控是各向异性的。当 y 方向偏振的电磁波垂直入射时，表现为由等效电感L以及等效电容C串联的LC电路；当 x 方向偏振的电磁波入射时，该结构可透过全部入射电磁波。这种反射式超构表面结构是一种高效率的宽带超构表面器件，反射效率接近100%。

由于等离激元纳米结构在光学范围内具有较高的本征欧姆损耗，器件效率难以提高，因此高折射率的全介质超构表面被用于实现高效率的纳米光子器件，代表性的结构是透射式介质柱(pillar)结构[图1(d)]。介质柱结构的机理是利用具有一定厚度的高介电常数的介质激发电磁波在厚度方向的Fabry-Pérot共振，进而引发相位和偏振的变化。如前述原理介绍，介质柱形状的变化对应传输相位的调控，介质柱的旋转则对应几何相位的调控[26]。

哈佛大学Capasso教授团队[31]通过传输相位和几何相位的联合调控，首次在单层全介质 TiO_2 纳米柱超构表面上实现了在任意一对偏振正交态上施加两个独立的任意相位轮廓，包括线偏振、圆偏振或椭圆偏振[图1(e)]。本团队通过复合自旋相关的几何相位和自旋无关的传输相位，打破了PSOI的对称性，提出了

非对称PSOI的概念，从而实现对LCP和RCP光的任意独立调控[24,41-43]。其基本原理为：由两对Si纳米柱组成的超级单元旋向相差π/4、传输相位相差π/2[图1(f)]，利用非对称PSOI实现自旋选择的干涉相消或相长，并通过纳米柱的空间旋转同时实现任意波前的调控[41]。基于该方法设计的超构表面，可通过单层结构同时实现高效的非对称传输(AT)和波前整形，有效解决圆偏振复用超构表面面临的能量利用率低、背景噪声大等原理性问题，而且为多功能集成器件、复杂光场调控等开辟了新思路。除了控制横截面的偏振外，全介质超构表面也实现了沿传播方向的偏振变换[44][图1(h)]。2021年，本团队证明了广义几何相位即具有高倍旋转对称性的超构原子可以实现等于数倍(传统为2倍)旋转角度的高阶几何相位[28,45][图1(g)]。

基于介质柱的传统偏振调控超构表面侧重于对庞加莱球表面某点对应的全偏振光的偏振态操控。最近，有研究团队设计并实验演示了用拓扑优化方法设计具有任意拓扑形状结构的超构表面，将非偏振的光束转换为具有任意偏振态和偏振度组合的光束[46][图1(i)]，即输出光束的偏振可以位于庞加莱球面上和面内的任意点。

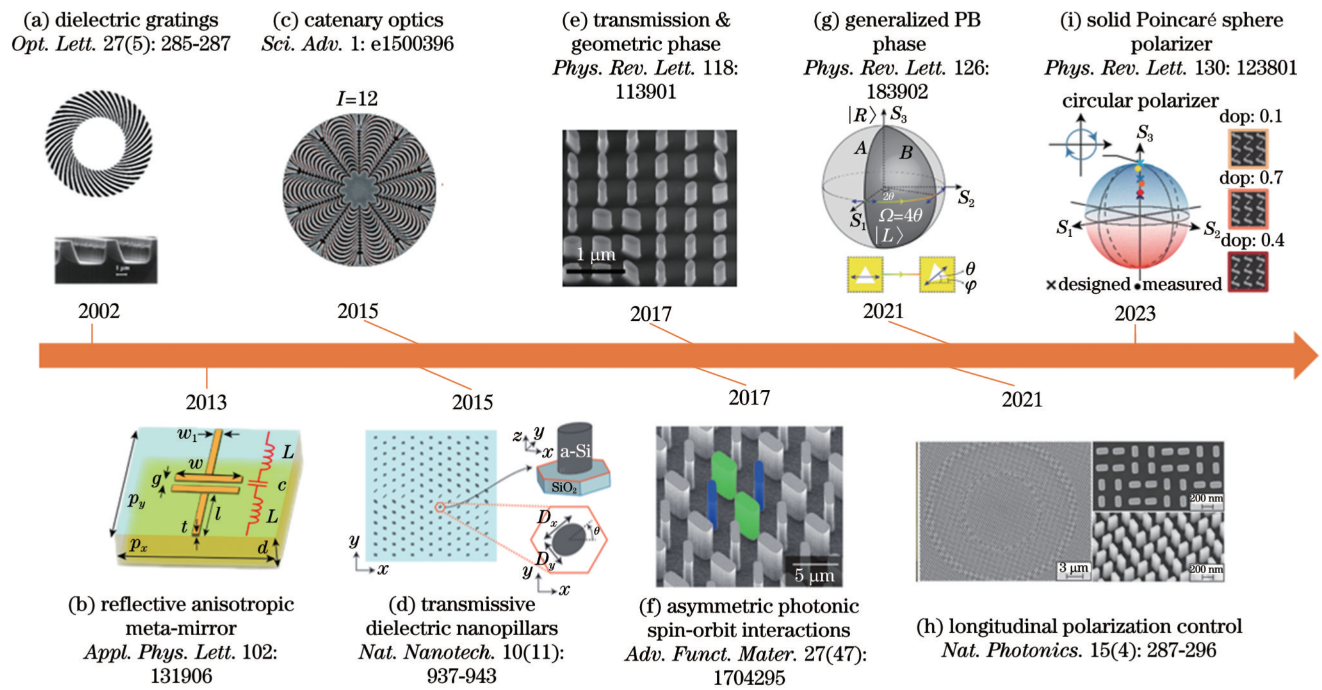

图1 电磁波偏振调控超构表面的典型结构发展路线图

Fig. 1 Roadmap of the metasurface for electromagnetic polarization manipulations

3 偏振调控超构表面的最新应用

偏振调控的应用范围非常广泛，在之前的综述[23,47]中已经多有阐述，本文主要介绍最近出现的一些新奇应用，如传输方向偏振转换器、矢量涡旋光束生成器、矢量全息和加密、矢量偏振测量和动态调控等。

3.1 传输方向偏振转换器

超构表面可以实现线偏振与圆偏振、椭圆偏振等不同偏振态的相互转换。通过各种巧妙的设计，目前已经在微波[48-49]、太赫兹[50-52]、光频段[53-54]实现了对电磁波偏振态的自由调控。例如，暨南大学李宝军教授团队利用一种具有4个自由度的最小数目的琼斯矩阵设计并构造出介质超构表面，从实验上证明了任意振幅、相位和偏振分布下两种光学状态之间的转换，而且这种任意转换可以在宽带波长范围和宽入射角范围内良好地运行[55]。另外一种全相位调制超构表面在圆偏振波入射下实现了对输出交叉极化分量和共极化分量的独立波前控制，然后叠加产生所需的偏振[56]。除了具有螺旋波前和光轴上一维(1D)偏振奇点的涡旋光场之外，心形片状二维(2D)奇异片也于2021年被设计出来[57]，在实验上表现为具有心形横截面的相位和极化奇异性。

除了常见的在横向平面控制偏振外，超构表面还可以在传输方向上实现纵向的偏振调控。2021年，哈佛大学Capasso教授团队[44]设计了一类新的基于超构表面的偏振片，实现了在传播方向上提供任意选择的偏振响应。如图2(a)、(b)所示，其原理是将入射波形转化为具有不同偏振态的准无衍射(铅笔状)光束的集合，这些光束沿着光轴拍频，从而在光传播过程中局部地改变偏振态，如同在各个z平面上受到串联的不同偏振器的作用。这种铅笔状光束还可以实现高保真度和低串扰的三维全息显示[58]。同样地，本团队基于非对称的光子自旋-轨道相互作用将偏振光学调控从二维空间扩展到三维空间[30][图2(c)~2(e)]。其内在机

制是通过非对称的光子自旋-轨道相互作用解耦两个正交偏振态，在横向和纵向空间中获得任意的相位和幅度差，从而在三维空间中随意地改变所产生的偏振分布。同时，通过实验获得了一个纵向变化的柱矢量场，该矢量场沿着传输方向，偏振分布在径向和角向偏振之间连续且周期性地切换[图 2(e)]。结合传输相位和几何相位的联合调控，天津大学姚建铨院士团队在太赫兹波段也获得了纵向变化的矢量涡旋光束[59]。

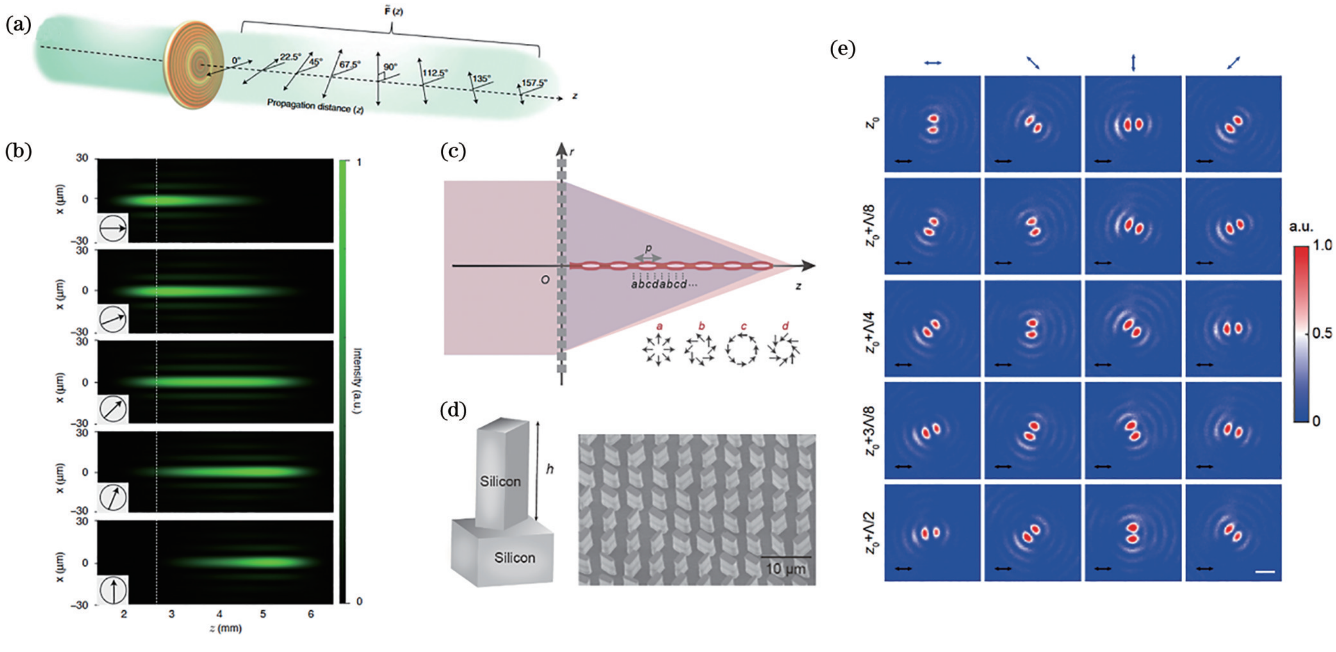

图 2 传输方向的偏振转换。(a)沿传播路径的偏振器件的原理图[44]；(b)所生成的铅笔状光束的纵向轮廓，插图为入射偏振，当输入偏振从 0°旋转到 90°时，轴上光强分布的质心不断远离光源[44]；(c)纵向变化的柱矢量光场的产生[30]；(d)单层超构表面的基本结构单元和扫描电子显微镜图像[30]；(e)不同入射偏振方向在不同 z 平面上测得的光强分布[30]，标尺：20 μm

Fig. 2 Polarization conversion along propagation direction. (a) A framework of the variable polarization optics along the propagation path[44]; (b) longitudinal patterns of the generated pencil-like beam for each incident polarization in the inset, the input shows the central point of on-axis intensity distribution moves further from the source when polarization is rotated from 0° to 90°[44]; (c) longitudinally variable cylindrical vector optical field generation[30]; (d) basic building blocks and SEM image of the monolayer metasurface[30]; (e) measured intensity profiles on various z-planes with different incident polarization orientations[30], scale bar: 20 μm

3.2 矢量涡旋光束生成器

携带轨道角动量(OAM)的光学涡旋由于其独特的光学特性和携带信息的额外自由度，在光学和光子学领域受到了广泛的关注。利用超构表面的偏振转换特性可以生成涡旋光束，其中矢量涡旋光束同时具有非均匀的偏振态并携带 OAM，在激光加工、光场操控等方面具有良好的应用前景[60]。相比于近来也被用于生成矢量涡旋光束的偏光全息术，超构表面具有更高的稳定性[61]。

2015 年，本团队[37]提出的连续线性变化的悬链线结构可实现宽带连续的几何相位调控，生成完美涡旋光束，其工作效率及带宽相对于传统离散型结构具有明显优势。所制备的拓扑荷数分别为−3、−6、12 的悬链线阵列的扫描电子显微镜图像[37]如图 3(a)～(c)第一列所示。在圆偏振光照明下，悬链线光阑同时产生两种强度近似相等的光束，一种是均匀相位光束，另一种是具有相反手性的螺旋相位光束[图 3(a)～(c)第二列]。由于干涉效应，该结构可以直接识别 OAM 的拓扑荷数。实验中采用 3 个波长分别为 532 nm、632.8 nm 和 780 nm 的激光光源来研究其宽带特性。图 3(a)～(c)的第三列展示了不同波长和偏振的实测强度图样，与矢量衍射理论得到的结果[图 3(a)～(c)第四列]一致，所生成的完美 OAM 光束证明了其优异的宽带消色差性能。进一步发展的变形悬链线结构，实现了巨大的光自旋霍尔效应角度[62]。除生成涡旋光束外，目前悬链线及准连续型结构还实现了多种高性能平面光学器件[62-67]，如平面透镜、贝塞尔光束生成器、彩色全息板等。

继生成完美涡旋光束之后，基于非对称 PSOI 原理设计的超构表面在 LCP/RCP 光入射下可生成任意独立拓扑荷的涡旋光束[68-69]，为生成矢量涡旋光束(完美矢量涡旋光束[70]、完美庞加莱光束[71]等)奠定了基础。

Capasso 教授团队[72]在传输方向的偏振调控基础上，进一步实现了自旋角动量(SAM)和 OAM 的同时独立控制。通过在任意两个指定的正交基之间切换输入偏振，一种基于光子总角动量(TAM)的器件产生了两个不同的空间可变涡旋光束[图 3(d)～(g)]。在这

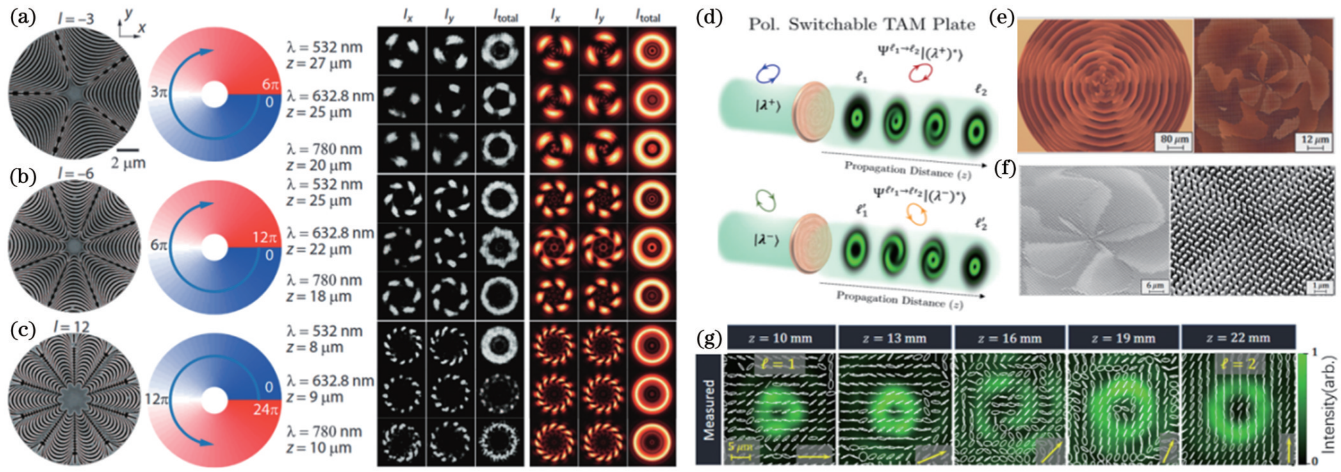

图3　涡旋光束生成器。(a)～(c)基于悬链线阵列的OAM生成器[37]；(d)～(g)偏振可切换的TAM板可以在3D空间中实现任意的自旋轨道耦合[72]

Fig. 3　Generator of vector vortex beam. (a)‒(c) OAM generators based on catenary arrays[37]; (d)‒(g) polarimetric switching TAM plate enables arbitrary spin-orbit coupling in 3D space[72]

种情况下，涡旋光束改变其OAM状态并沿z轴旋转其偏振态。这些器件的光学显微照片[图3(e)]显示了非常有特色的花瓣图案。这种多用途TAM板可以控制光的偏振和沿光路的OAM。

3.3　矢量全息和加密

全息术自发明以来，已成为塑造波前、记录和重建图像的重要技术。传统的全息术无法同时对空间偏振和相位分布进行调控，限制了各种全息复用的可能。通过设计超构表面中微纳结构的相位，实现精细的纳米级分辨率，从而编码全息复振幅，可以在指定平面上产生任意全息强度剖面，实现多通道全息显示。近年来，人们提出了一系列超构表面偏振调控的全息技术，包括偏振复用全息、矢量超构表面全息等，全息术在多通道显示、动态显示、数据存储和光学加密等领域有着广阔的应用前景[16,73-74]。

偏振复用全息得到了广泛的研究，例如：配备双相位全息图的介质超构表面实现了从一个全Stokes空间到另一个全Stokes空间的柔性偏振复用变换，可应用于时间序列全息显示和全Stokes偏振加密[75]；双波段工作的超构表面在紫外光照射下可观察到9幅偏振编码的全息图，而在可见光照射下出现了另一幅独立的全息图[76]。最近，南京大学彭茹雯、王牧教授团队[77]将光学响应噪声引入到琼斯矩阵元素的精确求解中，突破了超构表面偏振复用容量的物理极限[图4(a)]。通过理论和实验证实了在不同偏振的可见光照射下，利用单一超构表面可以获得多达11个独立偏振通道(11种线偏振态全息图像)，如图4(b)所示。结合位置复用方案，该超构表面可以产生36幅不同的图像，形成全息键盘图案，这为高容量光学显示、信息加密等应用提供了新思路。

矢量超构表面全息术可以同时控制成像平面上的强度和空间偏振分布，一般通过子阵列或交错纳米结构对重构图像的偏振态进行操控[78-81]。最近，单一线偏振光输入的矢量全息术也通过基于多原子超构分子和琼斯矩阵全息术的光学超构表面得到了证明[82-84]。基于几何相位超构表面对左、右旋圆偏振分量进行复振幅调控以及k空间调制，西北工业大学赵建林教授团队[84]提出一种可实现全偏振自由度调控彩色全息显示的超构表面器件。在非线性光学领域，南方科技大学李贵新教授课题组[85]通过具有三重旋转对称性的“双原子”超构单元，基于几何相位原理，对倍频光的相位、偏振和振幅进行调控，实现了任意偏振分布的非线性光学矢量全息成像。

在像素尺度上实现具有亚波长结构的全彩色矢量超全息图以及独立控制全息图像的空间偏振仍然是一个挑战。图4(c)演示了一种用于光学加密和动态显示的全彩色矢量全息投影[86]。该技术利用超构表面中3种不同尺寸硅纳米柱的交错，独立地操纵红(R)、绿(G)和蓝(B)光，通过选择入射和输出偏振态实现自由调谐全色全息图像的局部颜色和对比度，可以在像素尺度上直接控制RCP和LCP光的两幅重构图像的相位差，从而确定任意远场空间偏振态。

光学加密是矢量超构表面全息的重要应用方向，然而矢量光的空间变化偏振特性并没有在光学加密中得到很好的开发，导致了信息的安全性有限。最近，本团队提出了高安全性矢量可视密码学(visual cryptography)的概念，其密文是对自旋解耦双轴超透镜的矢量成像过程进行编码[87]。由于加密是与其他自由度(例如入射波长、偏振、OAM和自旋态的空间错位)相结合的，因此该方法具有更高的安全性。得益于基于超构表面的矢量光学操纵，复杂的加密过程可以通过一个紧凑的超相机进行反向解密[图4(d)]。

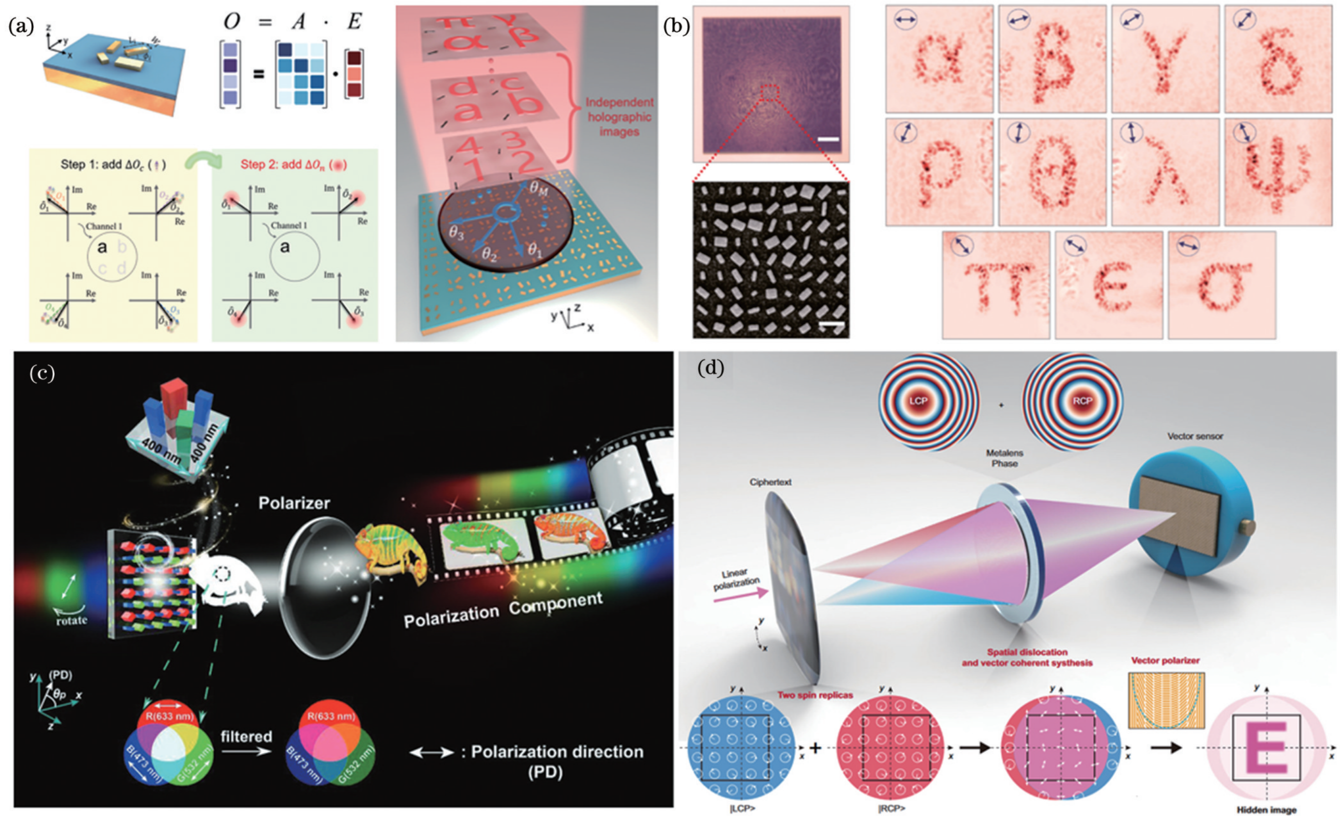

图 4 矢量全息与加密。(a)突破偏振复用容量极限的超构表面设计原理图[77]；(b)超构表面形貌图以及 11 种线偏振态全息图像的实验验证[77]；(c)用于光学加密和动态显示的全彩色矢量全息示意图[86]；(d)基于矢量可视密码学的元光学赋能的解密相机方案，解密相机由自旋解耦的双轴超透镜和矢量偏振传感器组成[87]

Fig. 4 Vectorial holography and encryption. (a) Metasurface design sketch for breaking the polarization multiplexing constraint[77]; (b) metasurface morphology and experimental demonstration of the holographic images at 11 linear polarization states[77]; (c) full-color vectorial holography for optical encryption and dynamic display[86]; (d) schematics of a meta-optics-empowered decryption camera for vector VC, which is composed of spin-decoupled dual-axis metalens and a vector polarization sensor[87]

一旦这些光学密钥参数完全匹配，隐藏的矢量光学信息就被转换成可检测的强度模式，从而可以在不需要额外测量和数字后处理的情况下实时地进行安全解密。

3.4 矢量偏振测量

在光与物质的相互作用中，偏振往往包含丰富的物质信息。在遥感[22]、光通信[88]、生物医学[89]等领域都需要应用偏振测量。全 Stokes 偏振测量法依赖于光束的 4 个 Stokes 参量的测量，因此传统的偏振测量方法需要对输入光进行至少 4 次强度测量。如果希望通过一次测量获得 Stokes 参数，则需要额外添加分束器、波片和起偏器等装置才能实现，这就限制了该方法在紧凑和集成光学系统中的应用。

具有强大的偏振操控能力的超构表面为偏振测量提供了新的途径。基于超构表面的偏振测量技术在过去的几年中引起了广泛的兴趣和研究，也已经开发出多种相关的偏振测量仪，如超紧凑偏振测量仪[90]、偏振成像[91-92]、Hartmann-Shack 波前传感器[93]和广角偏振测量[94]等。

虽然偏振测量仪的性能已经取得相当大的进展，但是仍然受到工作带宽窄和串扰大等问题的限制。本团队[95]通过偏振相关相位优化方法和粒子群优化算法精心设计并制备出一种由偏振敏感介质超透镜组成的无串扰、宽带消色差的全 Stokes 成像偏振测量仪。如图 5(a)所示，该偏振测量仪由 2×3 个子阵列组成，每个子阵列作为起偏器和消色差透镜。实验结果表明，所设计的偏振敏感超透镜可以有效地消除色差，降低串扰，保证了对偏振态更精确的测量，为生物光子学和集成光学等的广泛应用提供了一个很有潜力的平台。

宽带高精度的全 Stokes 偏振测量也可以通过深度学习算法来实现[96]。具体而言，该方法测量多个不同旋转角度介质手性壳超构表面的透射率，并根据深度学习算法预先建立的 Stokes 参数与记录透射率之间的映射关系，便可检测到 Stokes 参数[图 5(b)]。与传统的偏振测量仪相比，该方法的偏振探测精度对加工误差不敏感，在 400～840 nm 的宽波段范围内，Stokes 参数的平均均方误差小于 4%。

传统相机仅对强度敏感，而偏振成像获得的偏振信息可以揭示不可见的特征。哈佛大学 Capasso 教授

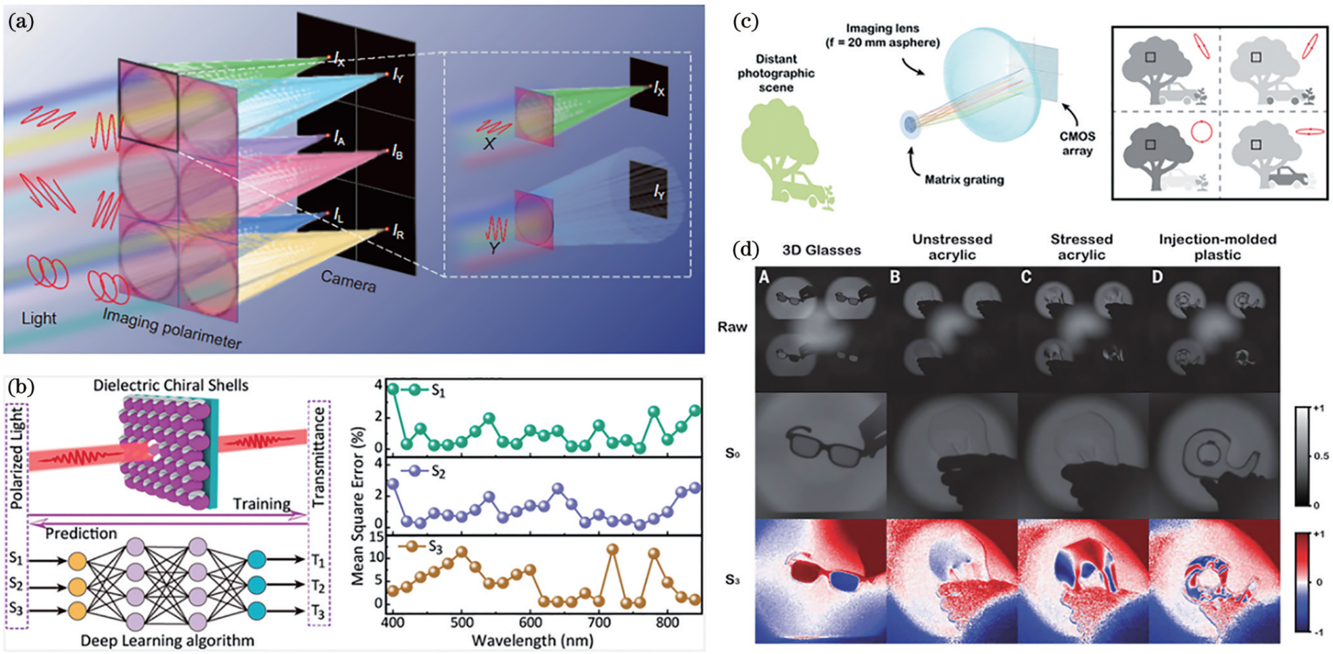

图 5　偏振测量与成像。(a)连续宽波段消色差偏振成像仪原理示意图[95]，右边虚线框显示了偏振相关相位优化的原理；(b)基于深度学习算法的高精度宽波段偏振计的工作原理图和宽带 Stokes参量探测性能[96]；(c)基于超构表面矩阵光栅的全 Stokes偏振相机的原理[91]；(d)利用测量的 Stokes参数 S_3实现偏振成像[91]

Fig. 5　Polarization measurement and imaging. (a) Continuous wide-band achromatic imaging polarimeter[95], the dashed box shows the principle of polarization dependent phase optimization; (b) schematic of high-precision wide-band polarimeter based on deep learning algorithm and broadband Stokes parameter detection performance[96]; (c) schematic of metagrating full Stokes polarization camera[91]; (d) polarization imaging makes use of the measured S_3 Stokes component[91]

团队[91]设计了一种基于超构表面矩阵光栅的全 Stokes偏振相机，可同时获得目标场景的二维图像信息和各点的偏振态信息。全 Stokes偏振相机的基本原理依赖于矩阵傅里叶光学，将平面波分解转换为 2×2的矩阵形式，允许矩阵中的每个平面波项由琼斯矩阵（而不是复标量）系数加权。矩阵光栅将输入光按照马吕斯定律分配到 4个衍射级上，每个衍射级分析远场中不同的偏振，从而采集到光的全偏振信息[图 5(c)]。将这种超光学元件与传统的互补金属氧化物半导体（CMOS）传感器集成，可以实时成像场景的空间偏振轮廓，使偏振敏感相机能够提供与原始强度图像相比的额外信息[图 5(d)]。此外，通过结合单层超透镜，还实现了单次拍摄获得包括目标场景的二维全焦强度、深度和偏振在内的四维图像的紧凑型相机[97]。

3.5　动态调控超构表面

动态超构表面是一种具有可调谐特性的超构表面，能够用于构建具有可重构或可编程功能的电磁器件，进而实现多功能系统智能化，例如无线通信加密[98]、动态全息投影[99]等，已成为近几年的研究热点[100]。最新研究结果显示，已制备出具有自我进化功能、形状可变的动态可编程超构表面[101]。

目前，设计动态超构表面的主要方法包括电学调控、温度调控和光学调控等[102-104]。采取在超构表面单元结构内集成开关二极管[105]、石墨烯[106]、相变材料[107]等可重构元件或材料的方式，可克服传统器件仅支持静态响应的缺点。

液晶在电场作用下会发生分子重新排列的现象，从而改变光的传播方式，是典型的电场响应的动态调制材料。当液晶与特殊设计的超构表面集成时，随着外部电场的变化，可实现宽带可见波长下入射光偏振的快速切换，从而显示出不同的全息图像。该超构表面由 Z形超构原子构成，其结构和工作原理如图 6(a)所示[108]。全息信息的相位掩模是采用动态相位调制和几何相位调制相结合的方法编码到超构表面的。另外，基于码分多路复用的超构表面全息编码方法，也实现了由波束形态和偏振态控制的动态全息图像[19]。

如果在可重构超构表面的极化调控中引入额外的时间维度编码，可获得动态操控电磁波的极化特征。2023年，南京大学的研究团队提出一种电磁波偏振动态调控的新方法——应用时空编码各向异性超构表面动态构建任意极化多波束[109]。通过超构表面各基本单元上独立加载的时空编码控制信号，可实现偏振态和散射方向图的联合调控，按需产生一系列具有任意偏振特性的远场多波束[图 6(b)]，该方法有望应用于诸如立体成像和无线通信等领域。

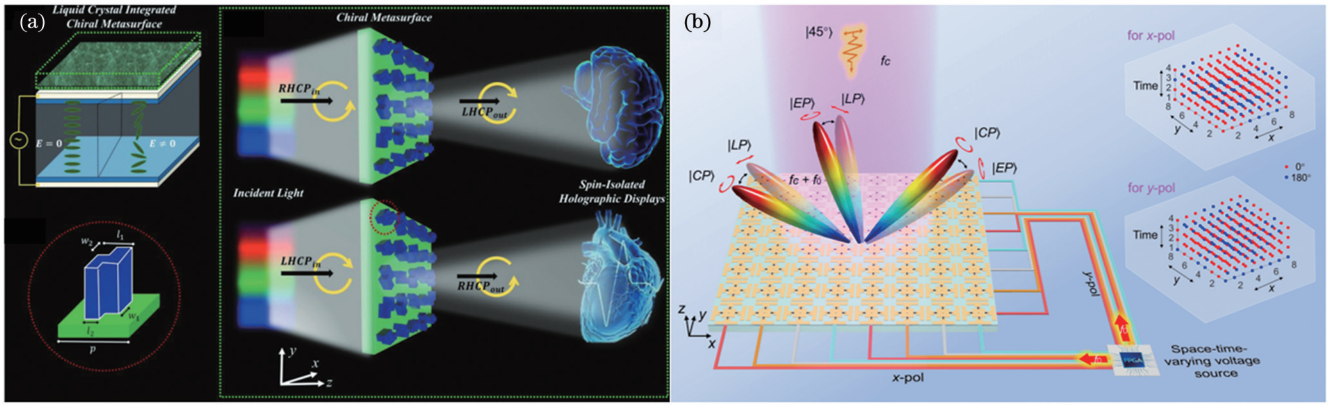

图 6 动态调控超构表面。(a)实现动态波前整形的电可调液晶集成的超构表面[108];(b)时空编码超构表面动态构建任意极化多波束的原理图[109]

Fig. 6 Dynamic metasurface platform. (a) Metasurface integrated with electrically adjustable liquid crystal to achieve dynamic wavefront shaping[108]; (b) framework of spatiotemporal coded metasurface for dynamic construction of arbitrarily polarized multi-beams[109]

4 总结与展望

电磁波偏振态的高效调控是电磁波操控的重要课题。超构表面由于其界面上各向异性的相位突变,可在亚波长尺度内实现对电磁波的逐点偏振转换和灵活波前调制,成为实现偏振调控和矢量光束生成的强大工具。超构表面兼具平面化和低损耗的优点,为实现轻量化和集成化光学系统提供有效的技术途径。基于超构表面偏振调控的应用研究在近年来得到了飞速发展,开发出一系列的功能器件和全新应用。本文总结了偏振调控超构表面在传播方向偏振转换、矢量涡旋光束生成等应用的最新进展。

偏振调控超构表面领域的未来发展还存在很多机遇和挑战,建议重点关注以下发展方向:

1) 深度学习赋能的超构表面设计。传统超构表面设计方法是基于正向设计的思路,存在设计复杂、功能单一、效率低等缺点。开发新型机器学习、深度学习等算法可以有效拓展设计思路、丰富功能、提高设计效率[110-111],进一步推动偏振调控超构表面领域的发展。

2) 除了在经典光学领域的应用,超构表面丰富的偏振操控能力还可以拓展到量子光学方面,包括光子统计、量子态叠加、量子纠缠和冷原子量子器件等[112-114]。这一新兴领域也是未来有潜力的发展方向。

3) 多功能集成化超构表面系统。现在超构表面已实现偏振、相位、振幅的多维度全方位调控,未来还可以与发射器、接收器、平面波导和光纤等经典光学器件集成,从而构建出超构表面系统来进行多功能电磁波调控,应用于空间波前控制[115-116]、偏振控制单光子发射器[117]、虚拟现实(VR)/增强现实(AR)显示[118-120]等。

参 考 文 献

[1] Pendry J B, Holden A J, Stewart W J, et al. Extremely low frequency plasmons in metallic mesostructures[J]. Physical Review Letters, 1996, 76(25): 4773-4776.

[2] Smith D R, Pendry J B, Wiltshire M C K. Metamaterials and negative refractive index[J]. Science, 2004, 305(5685): 788-792.

[3] Luo X G. Principles of electromagnetic waves in metasurfaces [J]. Science China Physics, Mechanics & Astronomy, 2015, 58 (9): 594201.

[4] Pendry J B, Schurig D, Smith D R. Controlling electromagnetic fields[J]. Science, 2006, 312(5781): 1780-1782.

[5] Liu K, Lin Z Y, Han B, et al. Non-volatile dynamically switchable color display via chalcogenide stepwise cavity resonators[J]. Opto-Electronic Advances, 2024, 7(1): 230033.

[6] Luo X G, Ishihara T. Surface plasmon resonant interference nanolithography technique[J]. Applied Physics Letters, 2004, 84 (23): 4780-4782.

[7] Gao P, Yao N, Wang C T, et al. Enhancing aspect profile of half-pitch 32 nm and 22 nm lithography with plasmonic cavity lens[J]. Applied Physics Letters, 2015, 106(9): 093110.

[8] Cao T, Lian M, Chen X Y, et al. Multi-cycle reconfigurable THz extraordinary optical transmission using chalcogenide metamaterials[J]. Opto-Electronic Science, 2022, 1(1): 210010.

[9] Pu M B, Zhao Z Y, Wang Y Q, et al. Spatially and spectrally engineered spin-orbit interaction for achromatic virtual shaping [J]. Scientific Reports, 2015, 5: 9822.

[10] Gigli C, Leo G. All-dielectric $\chi^{(2)}$ metasurfaces: recent progress [J]. Opto-Electronic Advances, 2022, 5(7): 210093.

[11] Fan J X, Li Z L, Xue Z Q, et al. Hybrid bound states in the continuum in terahertz metasurfaces[J]. Opto-Electronic Science, 2023, 2(4): 230006.

[12] Zhu R C, Wang J F, Qiu T S, et al. Direct field-to-pattern monolithic design of holographic metasurface via residual encoder -decoder convolutional neural network[J]. Opto-Electronic Advances, 2023, 6(8): 220148.

[13] Attiaoui A, Daligou G, Assali S, et al. Polarization-tuned fano resonances in all-dielectric short-wave infrared metasurface[J]. Advanced Materials, 2023, 35(28): e2300595.

[14] Buono W T, Forbes A. Nonlinear optics with structured light [J]. Opto-Electronic Advances, 2022, 5(6): 210174.

[15] Zhang Y X, Liu X F, Lin H, et al. Ultrafast multi-target control of tightly focused light fields[J]. Opto-Electronic Advances, 2022, 5(3): 210026.

[16] Zhao H, Wang X K, Liu S T, et al. Highly efficient vectorial field manipulation using a transmitted tri-layer metasurface in the terahertz band[J]. Opto-Electronic Advances, 2023, 6(2): 220012.

[17] Huang C X, Zhang J J, Cheng Q, et al. Polarization modulation for wireless communications based on metasurfaces[J]. Advanced Functional Materials, 2021, 31(36): 2103379.

[18] Zhang Y X, Jin J J, Pu M B, et al. Ultracompact metasurface

for simultaneous detection of polarization state and orbital angular momentum[J]. Laser & Photonics Reviews, 2024, 18(3): 2301012.

[19] Li X, Zhao R Z, Wei Q S, et al. Code division multiplexing inspired dynamic metasurface holography[J]. Advanced Functional Materials, 2021, 31(35): 2103326.

[20] Duan Y H, Zhang F, Pu M B, et al. Polarization-dependent spatial channel multiplexing dynamic hologram in the visible band[J]. Optics Express, 2021, 29(12): 18351-18361.

[21] Li X, Chen Q M, Zhang X, et al. Time-sequential color code division multiplexing holographic display with metasurface[J]. Opto-Electronic Advances, 2023, 6(8): 220060.

[22] Tyo J S, Goldstein D L, Chenault D B, et al. Review of passive imaging polarimetry for remote sensing applications[J]. Applied Optics, 2006, 45(22): 5453-5469.

[23] Hu Y Q, Wang X D, Luo X H, et al. All-dielectric metasurfaces for polarization manipulation: principles and emerging applications[J]. Nanophotonics, 2020, 9(12): 220.

[24] 张飞，郭迎辉，蒲明博，等.基于非对称光子自旋—轨道相互作用的超构表面[J].光电工程，2020，47(10): 200366.
Zhang F, Guo Y H, Pu M B, et al. Metasurfaces enabled by asymmetric photonic spin-orbit interactions[J]. Opto-Electronic Engineering, 2020, 47(10): 200366.

[25] 李雄，马晓亮，罗先刚.超表面相位调控原理及应用[J].光电工程，2017，44(3): 255-275.
Li X, Ma X L, Luo X G. Principles and applications of metasurfaces with phase modulation[J]. Opto-Electronic Engineering, 2017, 44(3): 255-275.

[26] Arbabi A, Horie Y, Bagheri M, et al. Dielectric metasurfaces for complete control of phase and polarization with subwavelength spatial resolution and high transmission[J]. Nature Nanotechnology, 2015, 10(11): 937-943.

[27] Ma X L, Pu M B, Li X, et al. All-metallic wide-angle metasurfaces for multifunctional polarization manipulation[J]. Opto-Electronic Advances, 2019, 2(3): 180023.

[28] Xie X, Pu M B, Jin J J, et al. Generalized Pancharatnam-Berry phase in rotationally symmetric meta-atoms[J]. Physical Review Letters, 2021, 126(18): 183902.

[29] Luo X G, Pu M B, Zhang F, et al. Vector optical field manipulation via structural functional materials: tutorial[J]. Journal of Applied Physics, 2022, 131(18): 181101.

[30] Zhang F, Pu M B, Guo Y H, et al. Synthetic vector optical fields with spatial and temporal tunability[J]. Science China Physics, Mechanics & Astronomy, 2022, 65(5): 254211.

[31] Balthasar Mueller J P, Rubin N A, Devlin R C, et al. Metasurface polarization optics: independent phase control of arbitrary orthogonal states of polarization[J]. Physical Review Letters, 2017, 118(11): 113901.

[32] Bomzon Z, Biener G, Kleiner V, et al. Space-variant Pancharatnam-Berry phase optical elements with computer-generated subwavelength gratings[J]. Optics Letters, 2002, 27(13): 1141-1143.

[33] Bomzon Z, Biener G, Kleiner V, et al. Radially and azimuthally polarized beams generated by space-variant dielectric subwavelength gratings[J]. Optics Letters, 2002, 27(5): 285-287.

[34] Bliokh K Y, Rodríguez-Fortuño F J, Nori F, et al. Spin-orbit interactions of light[J]. Nature Photonics, 2015, 9: 796-808.

[35] Liu S Q, Chen S Z, Wen S C, et al. Photonic spin Hall effect: fundamentals and emergent applications[J]. Opto-Electronic Science, 2022, 1(7): 220007.

[36] Chen W T, Yang K Y, Wang C M, et al. High-efficiency broadband meta-hologram with polarization-controlled dual images[J]. Nano Letters, 2014, 14(1): 225-230.

[37] Pu M B, Li X, Ma X L, et al. Catenary optics for achromatic generation of perfect optical angular momentum[J]. Science Advances, 2015, 1(9): e1500396.

[38] Hao J M, Zhou L, Chan C T. An effective-medium model for high-impedance surfaces[J]. Applied Physics A, 2007, 87(2): 281-284.

[39] Pu M B, Chen P, Wang Y Q, et al. Anisotropic meta-mirror for achromatic electromagnetic polarization manipulation[J]. Applied Physics Letters, 2013, 102(13): 131906.

[40] Grady N K, Heyes J E, Chowdhury D R, et al. Terahertz metamaterials for linear polarization conversion and anomalous refraction[J]. Science, 2013, 340(6138): 1304-1307.

[41] Zhang F, Pu M B, Li X, et al. All-dielectric metasurfaces for simultaneous giant circular asymmetric transmission and wavefront shaping based on asymmetric photonic spin-orbit interactions[J]. Advanced Functional Materials, 2017, 27(47): 1704295.

[42] Guo Y H, Pu M B, Zhao Z Y, et al. Merging geometric phase and plasmon retardation phase in continuously shaped metasurfaces for arbitrary orbital angular momentum generation[J]. ACS Photonics, 2016, 3(11): 2022-2029.

[43] Guo Y H, Zhang S C, Pu M B, et al. Spin-decoupled metasurface for simultaneous detection of spin and orbital angular momenta via momentum transformation[J]. Light: Science & Applications, 2021, 10: 63.

[44] Dorrah A H, Rubin N A, Zaidi A, et al. Metasurface optics for on-demand polarization transformations along the optical path[J]. Nature Photonics, 2021, 15: 287-296.

[45] Guo Y H, Pu M B, Zhang F, et al. Classical and generalized geometric phase in electromagnetic metasurfaces[J]. Photonics Insights, 2022, 1(1): R03.

[46] Wang S, Wen S, Deng Z L, et al. Metasurface-based solid Poincaré sphere polarizer[J]. Physical Review Letters, 2023, 130(12): 123801.

[47] 胡孟霞，王志强，李向平，等.超表面偏振信息编码[J].中国激光，2023，50(18): 1813010.
Hu M X, Wang Z Q, Li X P, et al. Metasurface polarization information encoding[J]. Chinese Journal of Lasers, 2023, 50(18): 1813010.

[48] Chen L, Ma Q, Nie Q F, et al. Dual-polarization programmable metasurface modulator for near-field information encoding and transmission[J]. Photonics Research, 2021, 9(2): 116-124.

[49] Li B Z, Chen Y H, Yu S L, et al. Ultra-thin broadband circular polarization conversion metasurface for full-space wavefront manipulation application[J]. IEEE Photonics Journal, 2023, 15(4): 4601009.

[50] Li J T, Wang G C, Yue Z, et al. Dynamic phase assembled terahertz metalens for reversible conversion between linear polarization and arbitrary circular polarization[J]. Opto-Electronic Advances, 2022, 5(1): 210062.

[51] Ren B, Feng Y X, Tang S, et al. Dynamic control of THz polarization modulation and multi-channel beam generation using a programmable metasurface[J]. Optics Express, 2021, 29(11): 17258-17268.

[52] Yue Z, Li J T, Li J, et al. Terahertz metasurface zone plates with arbitrary polarizations to a fixed polarization conversion[J]. Opto-Electronic Science, 2022, 1(3): 210014.

[53] Huang Y J, Xiao T X, Chen S, et al. All-optical controlled-NOT logic gate achieving directional asymmetric transmission based on metasurface doublet[J]. Opto-Electronic Advances, 2023, 6(7): 220073.

[54] Carletti L, Zilli A, Moia F, et al. Steering and encoding the polarization of the second harmonic in the visible with a monolithic $LiNbO_3$ metasurface[J]. ACS Photonics, 2021, 8(3): 731-737.

[55] Bao Y J, Weng Q, Li B J. Conversion between arbitrary amplitude, phase, and polarization with minimal degrees of freedom of metasurface[J]. Laser & Photonics Reviews, 2022, 16(2): 2100280.

[56] Yue Z, Li J T, Liu J Y, et al. Versatile polarization conversion and wavefront shaping based on fully phase-modulated

metasurface with complex amplitude modulation[J]. Advanced Optical Materials, 2022, 10(16): 2200733.

[57] Lim S W D, Park J S, Meretska M L, et al. Engineering phase and polarization singularity sheets[J]. Nature Communications, 2021, 12: 4190.

[58] Dorrah A H, Bordoloi P, de Angelis V S, et al. Light sheets for continuous-depth holography and three-dimensional volumetric displays[J]. Nature Photonics, 2023, 17: 427-434.

[59] Zheng C L, Li J, Liu J Y, et al. Creating longitudinally varying vector vortex beams with an all-dielectric metasurface[J]. Laser & Photonics Reviews, 2022, 16(10): 2200236.

[60] 柯岚, 章思梦, 李晨霞, 等. 超表面实现复杂矢量涡旋光束的研究进展[J]. 光电工程, 2023, 50(8): 230117.
Ke L, Zhang S M, Li C X, et al. Research progress on hybrid vector beam implementation by metasurfaces[J]. Opto-Electronic Engineering, 2023, 50(8): 230117.

[61] 郑淑君, 林枭, 黄志云, 等. 基于偏光全息的光场调控研究进展[J]. 光电工程, 2022, 49(11): 220114.
Zheng S J, Lin X, Huang Z Y, et al. Light field regulation based on polarization holography[J]. Opto-Electronic Engineering, 2022, 49(11): 220114.

[62] Luo X G, Pu M B, Li X, et al. Broadband spin Hall effect of light in single nanoapertures[J]. Light: Science & Applications, 2017, 6: e16276.

[63] Luo Z Y, Zhang W T, Song N N, et al. Fiber-integrated catenary ring-array metasurfaces for beam shaping[J]. Optics Letters, 2023, 48(1): 25-28.

[64] Wang D P, Hwang Y, Dai Y M, et al. Broadband high-efficiency chiral splitters and holograms from dielectric nanoarc metasurfaces[J]. Small, 2019, 15(20): e1900483.

[65] Guo Y H, Huang Y J, Li X, et al. Polarization-controlled broadband accelerating beams generation by single catenary-shaped metasurface[J]. Advanced Optical Materials, 2019, 7 (18): 1900503.

[66] Liu K P, Guo Y H, Pu M B, et al. Wide field-of-view and broadband terahertz beam steering based on gap plasmon geodesic antennas[J]. Scientific Reports, 2017, 7: 41642.

[67] Zhang F, Zeng Q Y, Pu M B, et al. Broadband and high-efficiency accelerating beam generation by dielectric catenary metasurfaces[J]. Nanophotonics, 2020, 9(9): 2829-2837.

[68] Zhang F, Pu M B, Luo J, et al. Symmetry breaking of photonic spin-orbit interactions in metasurfaces[J]. Opto-Electronic Engineering, 2017, 44(3): 319-325, 371.

[69] Devlin R C, Ambrosio A, Rubin N A, et al. Arbitrary spin-to-orbital angular momentum conversion of light[J]. Science, 2017, 358(6365): 896-901.

[70] Bao Y J, Ni J C, Qiu C W. A minimalist single-layer metasurface for arbitrary and full control of vector vortex beams [J]. Advanced Materials, 2020, 32(6): 1905659.

[71] Liu M Z, Huo P C, Zhu W Q, et al. Broadband generation of perfect Poincaré beams via dielectric spin-multiplexed metasurface[J]. Nature Communications, 2021, 12: 2230.

[72] Dorrah A H, Rubin N A, Tamagnone M, et al. Structuring total angular momentum of light along the propagation direction with polarization-controlled meta-optics[J]. Nature Communications, 2021, 12: 6249.

[73] Song Q H, Liu X S, Qiu C W, et al. Vectorial metasurface holography[J]. Applied Physics Reviews, 2022, 9(1): 011311.

[74] Deng Z L, Wang Z Q, Li F J, et al. Multi-freedom metasurface empowered vectorial holography[J]. Nanophotonics, 2022, 11 (9): 662.

[75] Zhang S F, Huang L L, Geng G Z, et al. Full-Stokes polarization transformations and time sequence metasurface holographic display[J]. Photonics Research, 2022, 10(4): 1031-1038.

[76] Kim J, Jeon D, Seong J, et al. Photonic encryption platform via dual-band vectorial metaholograms in the ultraviolet and visible [J]. ACS Nano, 2022, 16(3): 3546-3553.

[77] Xiong B, Liu Y, Xu Y H, et al. Breaking the limitation of polarization multiplexing in optical metasurfaces with engineered noise[J]. Science, 2023, 379(6629): 294-299.

[78] Deng Z L, Deng J H, Zhuang X, et al. Diatomic metasurface for vectorial holography[J]. Nano Letters, 2018, 18(5): 2885-2892.

[79] Song Q, Khadir S, Vézian S, et al. Bandwidth-unlimited polarization-maintaining metasurfaces[J]. Science Advances, 2021, 7(5): eabe1112.

[80] Zhang X Q, Yang S M, Yue W S, et al. Direct polarization measurement using a multiplexed Pancharatnam-Berry metahologram[J]. Optica, 2019, 6(9): 1190-1198.

[81] Song Q H, Baroni A, Wu P C, et al. Broadband decoupling of intensity and polarization with vectorial Fourier metasurfaces[J]. Nature Communications, 2021, 12: 3631.

[82] Yang H, Jiang Y T, Hu Y Q, et al. Noninterleaved metasurface for full-polarization three-dimensional vectorial holography[J]. Laser & Photonics Reviews, 2022, 16(11): 2200351.

[83] Kim I, Jang J, Kim G, et al. Pixelated bifunctional metasurface-driven dynamic vectorial holographic color prints for photonic security platform[J]. Nature Communications, 2021, 12: 3614.

[84] Guo X Y, Zhong J Z, Li B J, et al. Full-color holographic display and encryption with full-polarization degree of freedom [J]. Advanced Materials, 2022, 34(3): e2103192.

[85] Mao N B, Zhang G Q, Tang Y T, et al. Nonlinear vectorial holography with quad-atom metasurfaces[J]. Proceedings of the National Academy of Sciences of the United States of America, 2022, 119(22): e2204418119.

[86] Wan W P, Yang W H, Ye S, et al. Tunable full-color vectorial meta-holography[J]. Advanced Optical Materials, 2022, 10(22): 2201478.

[87] Zhang F, Guo Y H, Pu M B, et al. Meta-optics empowered vector visual cryptography for high security and rapid decryption [J]. Nature Communications, 2023, 14: 1946.

[88] Gaiarin S, Perego A M, da Silva E P, et al. Dual-polarization nonlinear Fourier transform-based optical communication system [J]. Optica, 2018, 5(3): 263-270.

[89] Garcia M, Edmiston C, Marinov R, et al. Bio-inspired color-polarization imager for real-time *in situ* imaging[J]. Optica, 2017, 4(10): 1263-1271.

[90] Balthasar Mueller J P, Leosson K, Capasso F. Ultracompact metasurface in-line polarimeter[J]. Optica, 2016, 3(1): 42-47.

[91] Rubin N A, D'Aversa G, Chevalier P, et al. Matrix Fourier optics enables a compact full-Stokes polarization camera[J]. Science, 2019, 365(6448): eaax1839.

[92] Xu C H, Ke C Z, Ma J, et al. Full-Stokes polarization imaging method based on the self-organized grating array in fused silica [J]. Scientific Reports, 2018, 8: 2331.

[93] Yang Z Y, Wang Z K, Wang Y X, et al. Generalized Hartmann-Shack array of dielectric metalens sub-arrays for polarimetric beam profiling[J]. Nature Communications, 2018, 9: 4607.

[94] Zhang Y X, Jin J J, Pu M B, et al. Full Stokes polarimetry for wide-angle incident light[J]. Physica Status Solidi Rapid Research Letters, 2020, 14(5): 2000044.

[95] Zhang Y X, Pu M B, Jin J J, et al. Crosstalk-free achromatic full Stokes imaging polarimetry metasurface enabled by polarization-dependent phase optimization[J]. Opto-Electronic Advances, 2022, 5(11): 220058.

[96] Xian S L, Huang S S, Qiu K H, et al. Highly precise and broadband full-Stokes polarimeter based on a deep learning algorithm[J]. ACS Photonics, 2023, 10(7): 2432-2439.

[97] Shen Z C, Zhao F, Jin C Q, et al. Monocular metasurface camera for passive single-shot 4D imaging[J]. Nature Communications, 2023, 14: 1035.

[98] Wang H L, Ma H F, Cui T J. A polarization-modulated information metasurface for encryption wireless communications [J]. Advanced Science, 2022, 9(34): e2204333.

[99] Yu P P, Liu Y F, Wu Y J, et al. Dynamic polarization holographic projection enabled by a scattering material-based reconfigurable hologram[J]. ACS Photonics, 2022, 9(11): 3712-3719.

[100] 黄晓俊, 高焕焕, 何嘉豪, 等. 动态可调谐的频域多功能可重构极化转换超表面[J]. 物理学报, 2022, 71(22): 224102.
Huang X J, Gao H H, He J H, et al. Dynamically tunable frequency-domain multifunctional reconfigurable polarization conversion metasurface[J]. Acta Physica Sinica, 2022, 71(22): 224102.

[101] Bai Y, Wang H L, Xue Y G, et al. A dynamically reprogrammable surface with self-evolving shape morphing[J]. Nature, 2022, 609(7928): 701-708.

[102] Gao H, Wang Y X, Fan X H, et al. Dynamic 3D metaholography in visible range with large frame number and high frame rate[J]. Science Advances, 2020, 6(28): eaba8595.

[103] Qu G Y, Yang W H, Song Q H, et al. Reprogrammable metahologram for optical encryption[J]. Nature Communications, 2020, 11: 5484.

[104] Wu P C, Sokhoyan R, Shirmanesh G K, et al. Near-infrared active metasurface for dynamic polarization conversion[J]. Advanced Optical Materials, 2021, 9(16): 2100230.

[105] Yang H, Wang S C, Li P, et al. A broadband multifunctional reconfigurable polarization conversion metasurface[J]. IEEE Transactions on Antennas and Propagation, 2023, 71(7): 5759-5767.

[106] Zeng C, Lu H, Mao D, et al. Graphene-empowered dynamic metasurfaces and metadevices[J]. Opto-Electronic Advances, 2022, 5(4): 200098.

[107] 史卓琳, 贺景琳, 王金金, 等. 基于相变材料GST的圆二色性可调谐外在手征超表面设计[J]. 光电工程, 2022, 49(10): 220092.
Shi Z L, He J L, Wang J J, et al. Design of tunable circular dichroism extrinsic chiral metasurface based on phase change material GST[J]. Opto-Electronic Engineering, 2022, 49(10): 220092.

[108] Naeem T, Kim J, Khaliq H S, et al. Dynamic chiral metasurfaces for broadband phase-gradient holographic displays [J]. Advanced Optical Materials, 2023, 11(5): 2202278.

[109] Hu Q, Yang W X, Wang J H, et al. Dynamically generating diverse multi-beams with on-demand polarizations through space-time coding metasurface[J]. Advanced Optical Materials, 2023: 2300093.

[110] Krasikov S, Tranter A, Bogdanov A, et al. Intelligent metaphotonics empowered by machine learning[J]. Opto-Electronic Advances, 2022, 5(3): 210147.

[111] Ma T G, Tobah M, Wang H Z, et al. Benchmarking deep learning-based models on nanophotonic inverse design problems [J]. Opto-Electronic Science, 2022, 1(1): 210012.

[112] Solntsev A S, Agarwal G S, Kivshar Y S. Metasurfaces for quantum photonics[J]. Nature Photonics, 2021, 15: 327-336.

[113] Liu J, Shi M Q, Chen Z, et al. Quantum photonics based on metasurfaces[J]. Opto-Electronic Advances, 2021, 4(9): 200092.

[114] Zhu L X, Liu X, Sain B, et al. A dielectric metasurface optical chip for the generation of cold atoms[J]. Science Advances, 2020, 6(31): eabb6667.

[115] Yu J, Park S, Hwang I, et al. Electrically tunable nonlinear polaritonic metasurface[J]. Nature Photonics, 2022, 16: 72-78.

[116] Iyer P P, DeCrescent R A, Mohtashami Y, et al. Unidirectional luminescence from InGaN/GaN quantum-well metasurfaces[J]. Nature Photonics, 2020, 14: 543-548.

[117] Kan Y H, Andersen S K H, Ding F, et al. Metasurface-enabled generation of circularly polarized single photons[J]. Advanced Materials, 2020, 32(16): e1907832.

[118] Li Z Y, Pestourie R, Park J S, et al. Inverse design enables large-scale high-performance meta-optics reshaping virtual reality [J]. Nature Communications, 2022, 13: 2409.

[119] Song J H, van de Groep J, Kim S J, et al. Non-local metasurfaces for spectrally decoupled wavefront manipulation and eye tracking [J]. Nature Nanotechnology, 2021, 16(11): 1224-1230.

[120] 李洋洋, 张超, 杨宁, 等. 超表面在增强现实近眼显示中的应用研究进展[J]. 激光与光电子学进展, 2022, 59(20): 2011005.
Li Y Y, Zhang C, Yang N, et al. Research progress on application of metasurface concept in augmented reality near-eye displays[J]. Laser & Optoelectronics Progress, 2022, 59(20): 2011005.

Recent Advances in Polarization Manipulation of Metasurfaces (Invited)

Xu Lijia[1,2,3], Zheng Yuhan[1,3,4,5], Guo Yinghui[1,3,4,5], Pu Mingbo[1,3,4,5], Li Xiong[1,3,4], Ma Xiaoliang[1,3,4], Luo Xiangang[1,3,4*]

[1]*State Key Laboratory of Optical Technologies on Nano-Fabrication and Micro-Engineering, Institute of Optics and Electronics, Chinese Academy of Sciences, Chengdu* 610209, *Sichuan, China*;

[2]*School of Automation Engineering, University of Electronic Science and Technology of China, Chengdu* 611731, *Sichuan, China*;

[3]*College of Materials Science and Opto-Electronic Technology, University of Chinese Academy of Sciences, Beijing* 100049, *China*;

[4]*National Key Laboratory of Optical Field Manipulation Science and Technology, Institute of Optics and Electronics, Chinese Academy of Sciences, Chengdu* 610209, *Sichuan, China*;

[5]*Research Center on Vector Optical Fields, Institute of Optics and Electronics, Chinese Academy of Sciences, Chengdu* 610209, *Sichuan, China*

Abstract

Significance Electromagnetic (EM) wave front modulation has significance for both scientific studies and industrial applications. However, traditional components for wave field manipulations are often bulky and heavy, which restricts their utilization in miniaturized optical devices and compact detection systems. Metasurfaces are usually composed of arrays of artificial microstructures, also known as meta-atoms, and arranged in a uniform or non-uniform spatial pattern. They can arbitrarily manipulate the amplitude, phase, and polarization of light with sub-wavelength resolution. As a result, metasurfaces have caught much attention in the research on next-generation optical systems. The metasurface design and fabrication has dramatically boosted the employment of optical field modification in compact optical equipment. Metasurfaces are anticipated to break through the bottleneck of conventional optical components and systems, paving the way for miniaturization, integration, and multifunctional processes. While traditional optical elements primarily regulate the optical field by phase accumulation of light along propagation, metasurfaces provide a novel method for controlling the optical field at subwavelength ranges via the interaction between light and meta-atoms. As a two-dimensional planar material with a thin depth profile, a metasurface can generate non-classical phase distributions for transmitted and reflected electromagnetic waves at its interface. Therefore, more flexible control over the wavefront can be realized. Polarization is an inherent property of light waves and electromagnetic waves. It comprises abundant information on substances, which is essential for target detection and identification. The efficient polarization state control is the core content of electromagnetic wave manipulation, which is vital for imaging, communication, display, optical encryption, and optical force manipulation. Due to its ability to manipulate the polarization state on the subwavelength scale, the metasurface serves as a powerful tool for polarization regulation and vector beam generation. Conventional polarization regulators such as those found in natural materials and three-dimensional superstructural materials typically control the global polarization of light by manipulating the amplitude and phase delay of the electric field in the orthogonal polarization components. In contrast, polarization and wavefront modulation by metasurface are the results of "abrupt phase changes" in anisotropic reflection/transmission at the interface. "Abrupt phase changes" mean a surface effect that depending on the mechanism can originate from the geometric (Pancharatnam Berry) phase, propagation phase, and generalized geometric phase. Artificially created meta-atoms can overcome the limitations of natural materials, like limited birefringence and polarization sensitivity. Acting as birefringent elements, the meta-atoms with specific designs can significantly enhance the polarization modulation capability, and be adopted to realize subwavelength pixelated polarization control for polarization conversion, polarization-dependent multiplexing and even generating complex vector beams. In recent years, polarization-modulated metasurfaces have drawn a lot of attention both in theory and applications, with continuously evolving new principles and applications. Thus, it is important to outline present research and emerging applications and thus better guide future development.

Progress We describe the basic principle and typical structure of metasurface design for polarization control, and then introduce and discuss the representative applications of metasurfaces, including polarization conversion along the propagation direction, vector vortex beam generation, vector holography and encryption, polarimeter, and dynamic control. In classic optics, the light polarization is commonly expressed mathematically by the Jones vector. Thus, the polarization control mechanism of metasurfaces is explained by solving Jones matrix. The roadmap of electromagnetic polarization manipulations with metasurfaces is summarized in Fig. 1. The two important mechanisms for metasurfaces to control polarization are the geometric phase and the propagation phase. The geometric phase for anisotropic materials is solely determined by the rotation angle θ as it results from the photonic spin-orbit interaction (PSOI). The propagation phase is related to the shape and size of the structure. Recently, our research group has proposed a novel principle of metasurfaces to break the PSOI symmetry by merging the geometric phase and propagation phase. We also summarize some emerging applications of polarization modulation by metasurfaces, involving polarization conversion along propagation direction, vector vortex beam generation, vector holography and encryption, polarimeter, and dynamic control. Meanwhile, we elaborate on the ideas of each study, analyze their advantages and limitations, and discuss their prospective implementations. For example, in addition to controlling polarization in the transverse plane, a new class of metasurfaces achieves parallel polarization transformations along the optical path. In this case, a single metasurface can mimic an arrangement of multiple polarization optics cascaded in series. By employing the polarization-dependent phase optimization concept, our group has reported a crosstalk-free broadband achromatic full Stokes imaging polarimeter composed of polarization-sensitive dielectric metalenses. The average crosstalk under incident light with arbitrary polarization has been largely reduced to ensure a more precise measurement of the polarization state. Finally, the challenges and future development direction of polarization-modulated metasurfaces and the areas are also prospected.

Conclusions and Prospects In summary, we highlight the promising polarization-related applications for metasurfaces and serve as up-to-date references for researchers in metasurface and metamaterial fields. As a new generation of transformative optical devices, polarization-modulated metasurfaces will provide a broad platform for polarization conversion, vector vortex beam generation, vector holography and encryption, polarimeter, *etc*.

Key words physical optics; metasurface; vortex beam; polarization; holography; polarimeter; dynamic control